(Received 24 August 2025, Accepted 31 October 2025, Scheduled 16 November 2025)

A Broadband Circularly Polarized Aperture-Coupled Magneto-Electric Dipole

Yanhong Xu[1,*], Haoxiang Li[1], Weiwei Wang[2], Nanyue Li[1], Xuhui Fan[1], and Jianqiang Hou[3]

[1]*Xi'an Key Laboratory of Network Convergence Communication College of Communication and Information Engineering Xi'an University of Science and Technology, Xi'an 710054, China*
[2]*China Academy of Space Technology Xi'an, Xi'an 710100, China*
[3]*National Key Laboratory of Science and Technology on Antenna and Microwave Xidian University, Xi'an 710071, China*

ABSTRACT: In this paper, a broadband circularly polarized (CP) magneto-electric (ME) dipole antenna based on a microstrip line aperture-coupled feeding structure is proposed. The antenna is fed by the microstrip line, which is utilized to couple the energy to the antenna through the slot etched on the ground plane. Based on a linearly polarized (LP) ME dipole antenna, two centrosymmetric L-shaped strips are loaded to the patches located at the $+45^\circ$ diagonal position, and the patches located at the -45° diagonal position are truncated. As a result, the current direction is changed to be parallel to the equivalent magnetic current to radiate CP wave. To improve the axial-ratio (AR) bandwidth of the antenna, the rectangular slot initially etched on the ground plane is modified to an asymmetric cross slot, which can generate a minimum AR point at high frequency. In this way, the AR bandwidth is increased from 32.4% to 51.7%. On this basis, to further extend the AR bandwidth, the metal columns are introduced at both ends of the antenna, and another additional AR minimum point is generated at the low frequency. The measured results indicate that the impedance bandwidth ($|S_{11}| \leq -10$ dB) is 57% (2.40–4.33 GHz), and the 3 dB AR bandwidth is 63% (2.39–4.57 GHz). Moreover, the proposed antenna exhibits flat gain and stable unidirectional radiation pattern across the operational frequency region.

1. INTRODUCTION

In the past decade, circularly polarized (CP) antennas have been widely investigated [1–11] due to the advantages of suppressing multipath loss and reducing polarization mismatch. With the rapid development of modern wireless communication systems, higher requirements for antenna stability and reliability are presented, so CP antennas need wider impedance bandwidth, axial-ratio (AR) bandwidth, and stable gain [12]. Based on the concept of complementary antenna, Luk and Wong first proposed a magneto-electric (ME) dipole antenna in 2006 [13]. The antenna is composed of a pair of orthogonally placed electric dipole and magnetic dipole. By combining orthogonal dipoles, excellent antenna characteristics can be achieved such as wide impedance bandwidth, low back radiation, high gain, and stable radiation pattern [14–16].

Due to above excellent properties, various types of CP ME dipoles have been proposed in recent years [17–26]. The typical design methods of CP ME dipoles can be divided into single feed and dual feed. The antenna with single feed is generally simple in structure, but the AR bandwidth is narrow [17, 18], while the antenna with dual feed can achieve wider AR bandwidth at the expense of a complex feeding network [19, 20]. Therefore, the design of a CP ME dipole antenna with a simple structure and wide AR bandwidth is very challenging to the communication system. In [21], by changing the shape and size of a linearly polarized (LP) antenna, a broadband CP antenna fed by an L-shaped probe is designed, and finally a 47.7% wide AR bandwidth can be achieved. However, this feed has high requirements for processing and measurement. The microstrip line aperture-coupled feeding method is used in [22] to replace the traditional probe feed to excite the CP ME dipole antenna, which reduced the feed complexity. In addition, a metal strip is introduced at diagonal position to connect the two patches of the antenna, which can excite another ME dipole mode in the orthogonal direction to generate CP radiation, but the AR bandwidth is only 22.5%. In order to expand the AR bandwidth while maintaining the simplicity of antenna structure, it is a common method to change the shape of the electric dipole. In [23], by loading an F-shaped strip on the electric dipole to change the current direction and truncating the partial patch to further improve the AR performance, a 3 dB AR bandwidth of 32% is finally achieved. A bow-tie patch is used as the radiator in [24] instead of the traditional rectangular patch, so that the radiation field amplitude of the electric dipole and magnetic dipole is balanced to obtain good CP performance (36.6%). Loading a resonant structure is also an effective way to expand AR bandwidth. By loading two rows of arc-shaped vias at both ends of the magnetic dipole in [25], the direction of the magnetic current can be changed to compensate the deviation of the current direction with the frequency. The AR bandwidth

* Corresponding author: Yanhong Xu (yanhongxuxidian@163.com).

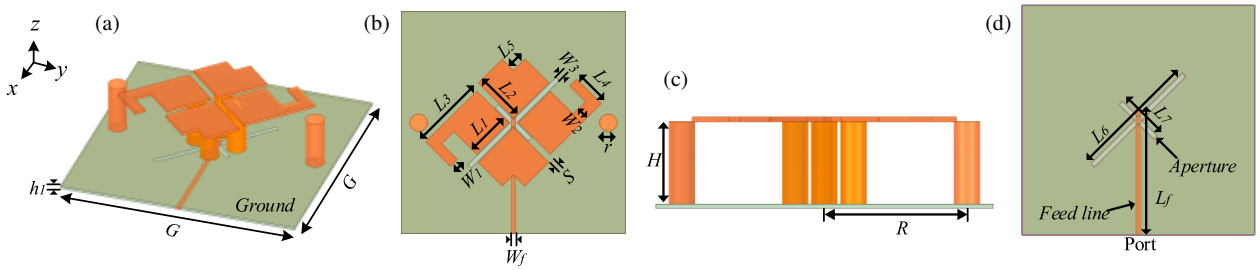

FIGURE 1. Structure of proposed ME dipole antenna. (a) Perspective view. (b) Zoomed-in top view. (c) Side view. (d) Zoomed-in view of feeding structure. ($G = 90$, $h_1 = 1$, $H = 18.5$, $L_1 = 18$, $L_2 = 20$, $L_3 = 29$, $L_4 = 14$, $L_5 = 6.5$, $L_6 = 50$, $L_7 = 19$, $L_f = 50$, $W_1 = 4$, $W_2 = 5$, $W_3 = 1.8$, $W_f = 1.9$, $S = 2.8$, $r = 7$, $R = 38$ in mm).

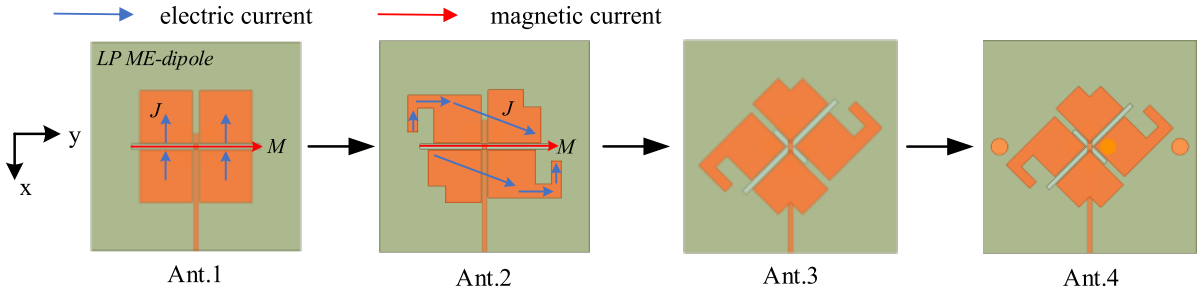

FIGURE 2. Design process of the proposed CP antenna element.

of the antenna is extended to 40.9%. In [26], by introducing a parasitic ring that is coplanar with the horizontal patches, different CP modes are combined to increase the AR bandwidth by 42.1%.

In this paper, a broadband CP ME dipole antenna with simple feed is proposed. In order to improve the AR bandwidth without increasing the size and complexity of antenna structure, an asymmetric cross slot structure loaded on the ground is first used to widen the AR bandwidth at high frequency. Then, the metal columns on both sides of the antenna are designed to further expand the AR bandwidth at low frequencies. The measured results show that the proposed antenna owns a wide impedance bandwidth of 57% (2.40–4.33 GHz) and a 3 dB AR bandwidth of 63% (2.39–4.57 GHz). Besides, the antenna is simple in structure and easy to fabricate. For verifying, the design details, fabrication, and measurement results of the antenna are given.

2. ANTENNA DESIGNS AND ANALYSIS

2.1. Antenna Structure

The geometric structure of the proposed antenna is shown in Figure 1. It is composed of two pairs of vertically placed ME dipoles, two pairs of metal columns, and a ground plane etched with a slot. A 1 mm thick FR4 substrate with $\varepsilon_r = 4.4$ and $\tan\delta = 0.02$ is used. The upper surface of the substrate is covered with a ground plane, and an asymmetric cross slot is etched on it. A microstrip feedline is printed at the bottom to couple the energy to the antenna. For the radiation part, the electric dipole is composed of four square patches on the horizontal plane. L-shaped strips and truncated parts are loaded at the diagonal of the two pairs of patches to complete the transformation of the antenna from LP to CP. Each patch is connected to the ground plane by a metal column, so the equivalent magnetic dipole is realized by the aperture between the patches. The whole radiator is rotated by 45° in order to avoid direct contact with the slot. Finally, a pair of metal columns is introduced at the left and right sides of the antenna along the y-axis.

2.2. Design Process

In order to understand the CP mechanism, the design process of the proposed antenna is plotted in Figure 2. Figure 3 shows the simulated $|S_{11}|$ and AR of Ant. 1–Ant. 4. There are four steps in total.

Step 1: an LP ME dipole antenna with a center frequency of 3.75 GHz is first designed where the horizontal patches act as the electric dipole, while the aperture between shorted patches is equivalent to the magnetic dipole. According to the design principle of [13], the initial patch length L_1 and height H are $\lambda_0/4$ for the best resonance characteristic (λ_0 is the free-space wavelength at 3.75 GHz). At this time, the current on the electric dipole is along the x-axis direction, and the equivalent magnetic current introduced by the magnetic dipole is along the y-axis direction. Therefore, the LP radiation is excited. The $|S_{11}|$ of the designed LP ME dipole is shown in Figure 3.

Step 2: To realize CP radiation, the current **J** must be parallel to the equivalent magnetic current **M**. On the basis of Ant. 1, two centrosymmetric L-shaped strips are loaded to the patches located at the $+45°$ diagonal position and the patches located at the $-45°$ diagonal position are truncated. By the superposition of current perturbations, the current will be deflected, which can be parallel to the magnetic current. Due to the same excitation amplitude, CP waves are generated. The optimized Ant. 2 can generate two minimum AR points, and a 32.4% AR band-

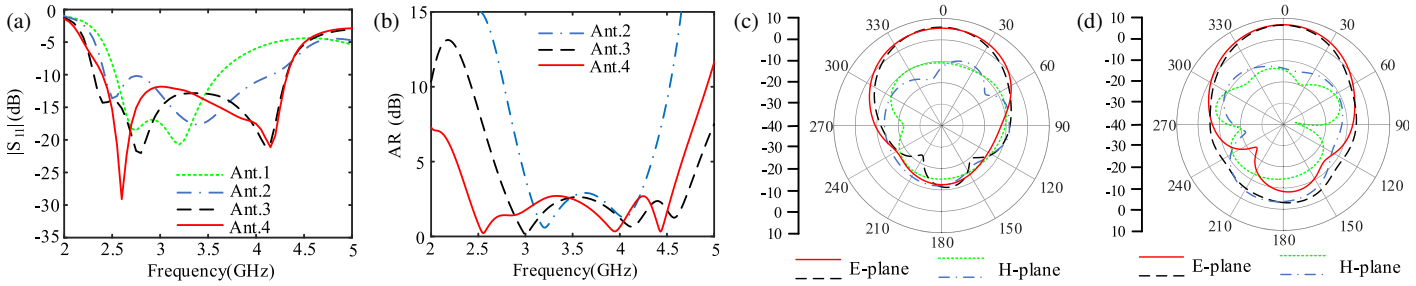

FIGURE 3. Simulated results of different evolution antennas. (a) Reflection coefficient. (b) Axial ratio. (c) Radiation patterns of Ant. 2 at 3.5 GHz. (d) Radiation patterns of Ant. 4 at 3.5 GHz.

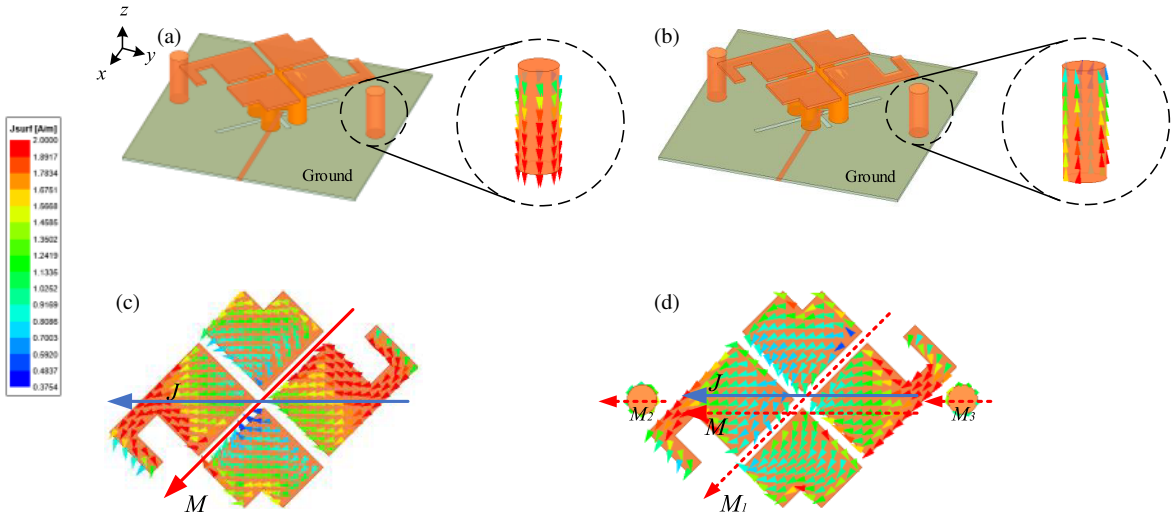

FIGURE 4. Simulated surface current distribution. (a) Inner side of the metal columns. (b) Outer side of the metal columns. (c) The patch without metal columns at 2.5 GHz. (d) The patch with metal columns at 2.5 GHz.

width is achieved. However, the AR bandwidth of Ant. 2 is still narrow.

Step 3: To improve the CP performance of Ant. 2, a composite CP method is used. The rectangular slot etched on the ground plane is changed to an asymmetric cross slot. For wideband operation, slot length L_7 is initially $\lambda_0/2$ to ensure efficient energy coupling. Subsequently, it is optimized to 19 mm to improve the CP performance at high frequencies. The structure of Ant. 2 is capable of radiating CP waves, and the feeding slot can also be excited with two degenerate modes to radiate CP waves. Combining these two methods, the AR bandwidth of the antenna is significantly improved. As shown in Figure 3, the AR bandwidth of Ant. 3 is broadened to 51.7%.

Step 4: To further extend the AR bandwidth, a pair of metal column is introduced on both sides of the antenna. Figures 3(c) and (d) show radiation patterns of the antenna before and after introducing the slot and metal columns at 3.5 GHz. The patterns exhibit only minor differences in cross-polarization levels, phase center and front-to-back ratio, demonstrating that the proposed antenna can effectively maintain stable radiation characteristics while enhancing bandwidth.

In order to illustrate the function of the metal columns, the surface current distributions on the inner side and outer side of the metal columns is shown in Figures 4(a) and (b). Due to the centrosymmetric of antenna structure, only those on one side are given. It can be seen that the current on the inner surface of the metal column is along the $-z$-axis direction while that on the outer surface is along the $+z$-axis direction. The opposite directions of the surface currents on two sides of the same metal column will cause them to offset each other, so the electrical current will not be generated to affect the electric dipole. The change in the direction of the magnetic current caused by the metal column can compensate the deviation of electrical current direction with frequency, so that the direction of the total magnetic current can be parallel to the total electrical current in a lower frequency. Therefore, the AR bandwidth is extended to a lower frequency. To further solidify the mechanism, the vector current distributions on the patch with and without metal columns at 2.5 GHz are shown in Figures 4(c) and (d). Without metal columns, the electric current **J** deviates from the equivalent magnetic current which is combined with $\mathbf{M}_2$, $\mathbf{M}_3$ to form a total magnetic current **M**, reducing the angle between **J** and **M**. This restores the CP condition, generating an additional AR minimum point at low frequencies.

2.3. Principle of Operation

To illustrate the working principle of the proposed antenna, Figure 5 shows current distribution of the antenna at $t = 0, T/4, T/2$ and $3T/4$, where T is the period of oscillation at 2.6 GHz. Since Ant. 3 rotates on the basis of Ant. 2, a new

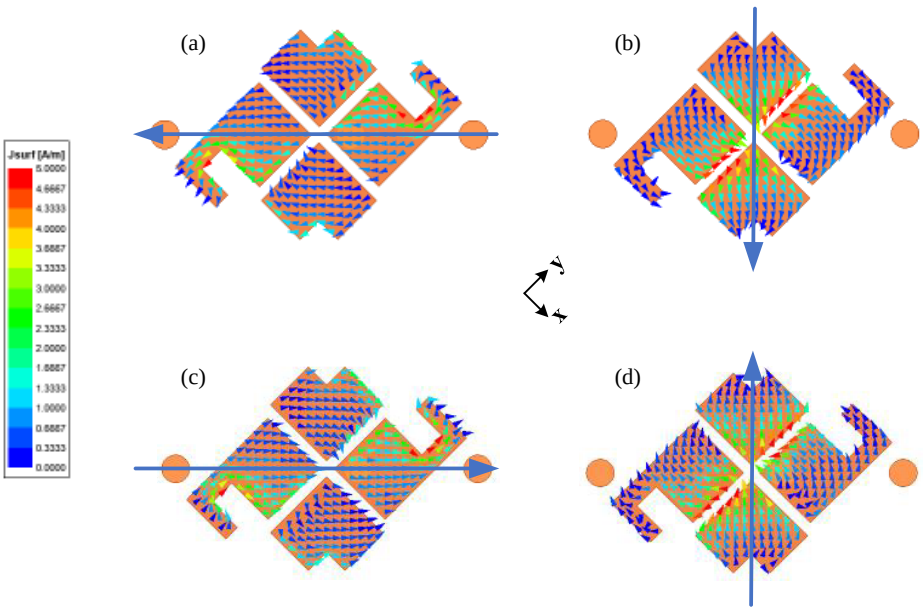

FIGURE 5. Electrical current distributions on the electric dipole over a period of time. (a) $t = 0$, (b) $t = T/4$, (c) $t = T/2$, (d) $t = 3T/4$.

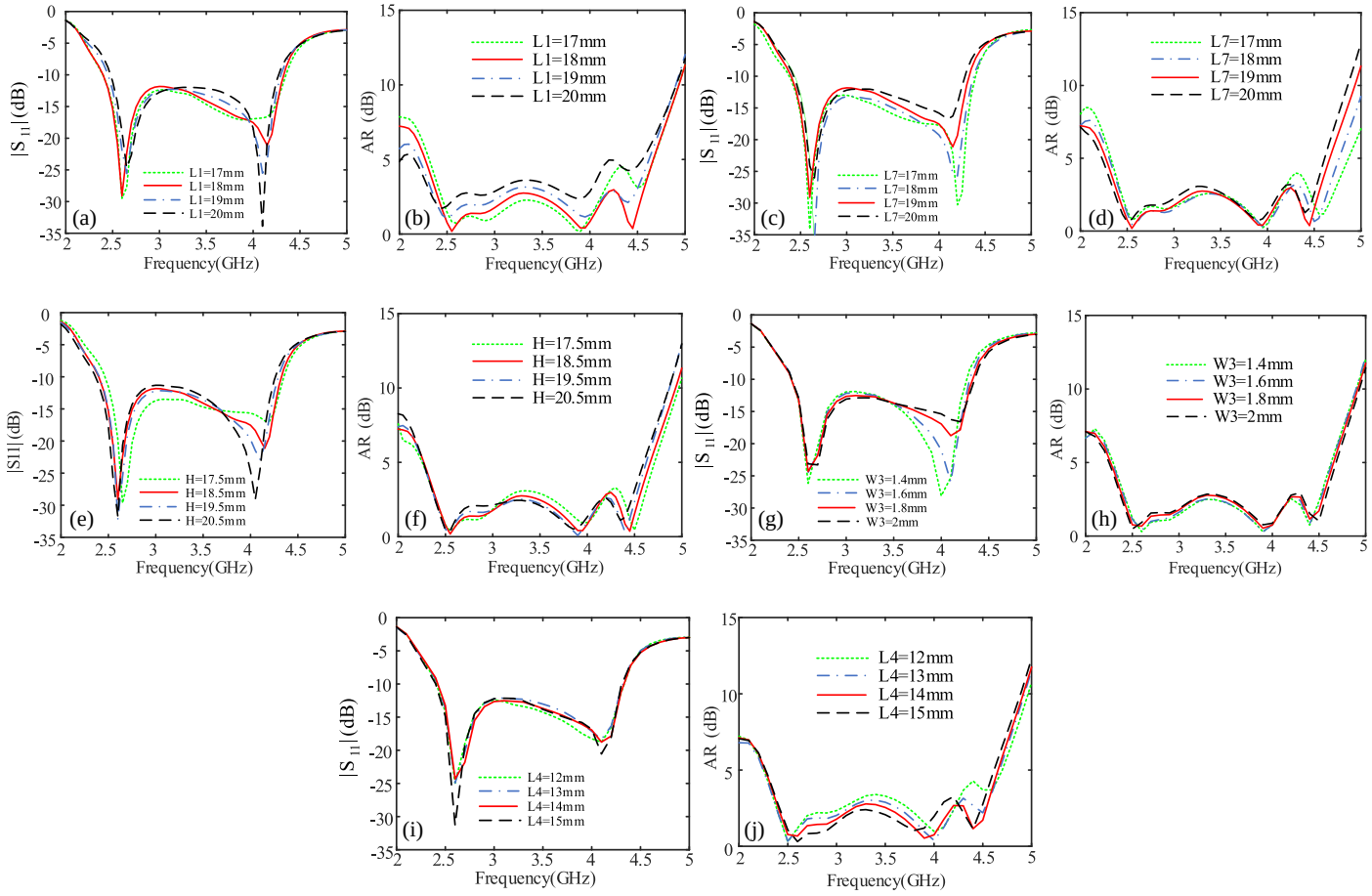

FIGURE 6. Simulated results of the proposed antenna with different values. (a) Effects of L_1 on $|S_{11}|$. (b) Effects of L_1 on AR. (c) Effects of L_7 on $|S_{11}|$. (d) Effects of L_7 on AR. (e) Effects of H on $|S_{11}|$. (f) Effects of H on AR. (g) Effects of W_3 on $|S_{11}|$. (h) Effects of W_3 on AR. (i) Effects of L_4 on $|S_{11}|$. (j) Effects of L_4 on AR.

coordinate axis with the counterclockwise rotation of 45° is established. After optimizing Ant. 2 to Ant. 3, the current **J** and equivalent magnetic current **M** of the antenna are along the $+45°$ and $-45°$ directions. This makes it difficult to visually distinguish the direction relationship between **J** and **M** in the original coordinate system. In the new coordinate system with a

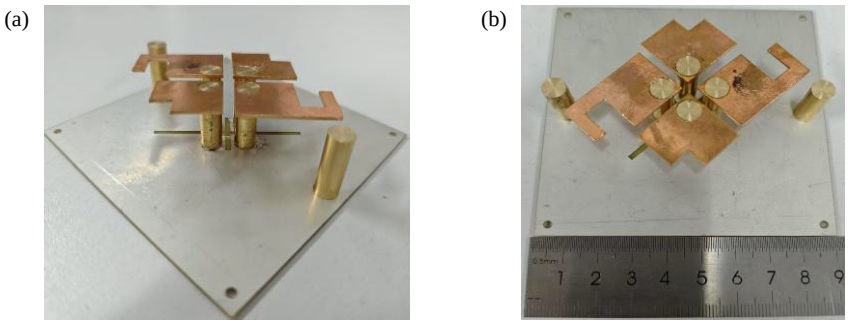

FIGURE 7. Photograph of the fabricated antenna. (a) Perspective view. (b) Top view.

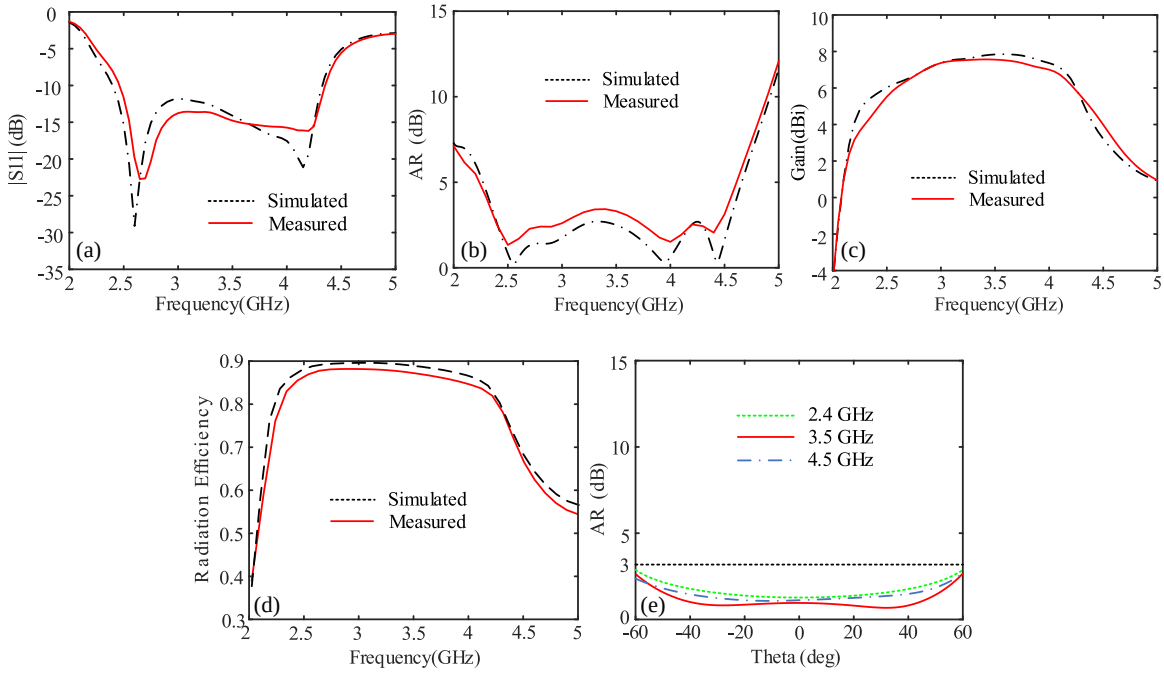

FIGURE 8. Simulated and measured results of the proposed antenna. (a) $|S_{11}|$. (b) AR. (c) Gain. (d) Radiation Efficiency. (e) AR at different angles.

rotation of 45°, the y axis is parallel to the directions of **J** and **M**, which makes it more intuitive to observe whether the antenna meets the CP radiation conditions. At $t = 0$ and $T/2$, the currents on the edge of the planar electric dipole reach maximum and are in opposite directions for the two times, which means that the electric dipole along the y-axis direction is strongly excited. When $t = T/4$ and $3T/4$, the currents on the aperture reaches maximum and are in opposite directions, indicating that the equivalent magnetic current from the patch aperture is also along the y-axis. Therefore, the electric dipole and magnetic dipole are excited in parallel with a phase difference of 90°, and CP radiation is achieved. It can be seen that as the time varies, the electrical current on the electric dipole rotates in counterclockwise direction. Therefore, a right-hand CP (RHCP) wave is generated.

In order to further study the working principle of the proposed antenna, a parametric analysis is conducted by using Ansys HFSS based on finite element method (FEM). The influence of the patch length L_1 on the simulated $|S_{11}|$ and AR is analyzed first. By analyzing Figures 6(a) and (b), it can be seen that the change of L_1 has little effect on the impedance matching of the antenna. The resonant frequency at high frequency moves toward the low frequency as L_1 increases. At the same time, the CP performance first becomes better and then worse. The influence of the slot length L_7 on the simulated $|S_{11}|$ and AR is also shown in Figures 6(c) and (d). It can be seen that the change of L_7 has a great influence on the high frequency resonance point. The current path will be extended as L_7 increases, and the impedance matching of the high frequency begins to deteriorate. For AR, the minimum AR point at 4.4 GHz is generated by the slot etched on the ground plane, so the high frequency is also sensitive to the change of L_7. The influence of the metal column height H on the simulated $|S_{11}|$ and AR is shown in Figures 6(e) and (f). When H increases, the $|S_{11}|$ and AR curves move to the low frequency as a whole. Although a wider AR can be obtained, the impedance matching becomes worse. Figures 6(g) and (h) show the influence of asymmetric cross-slot width W_3 on the simulated $|S_{11}|$ and AR. It can be

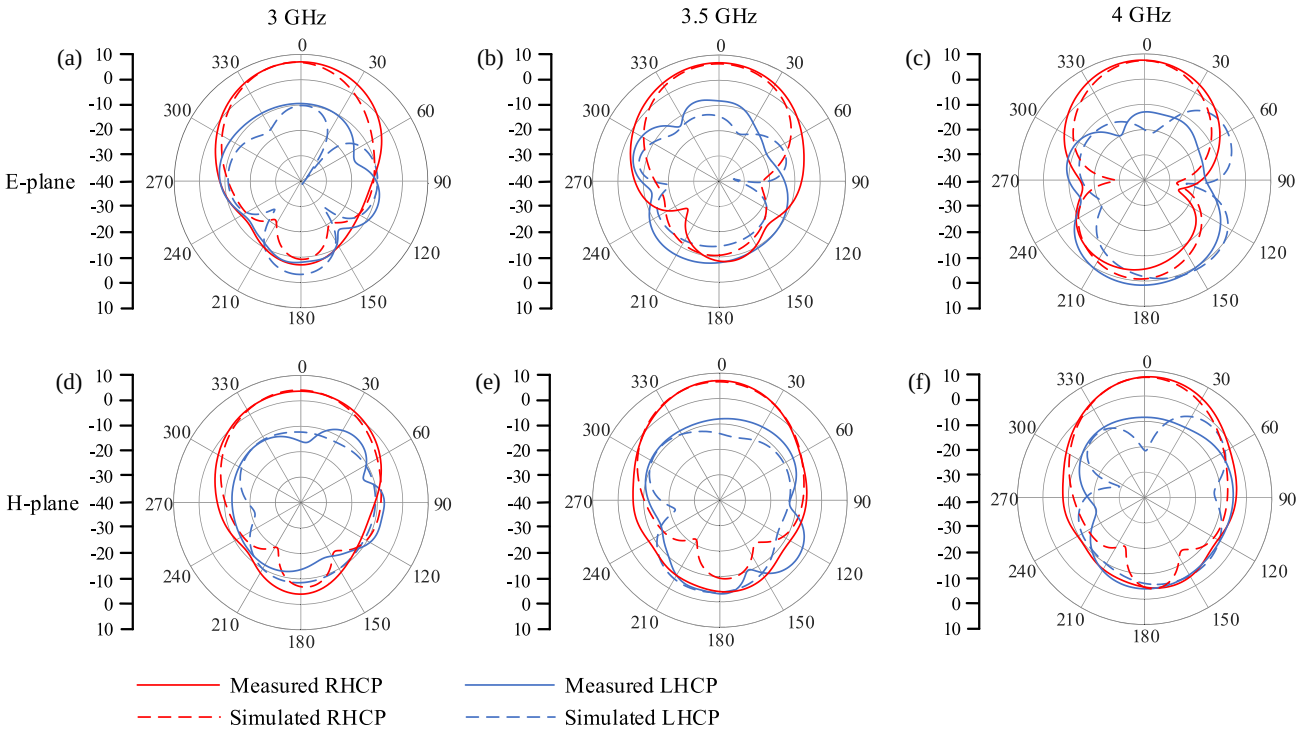

FIGURE 9. Simulated and measured radiation patterns at (a) 3, (b) 3.5, and (c) 4 GHz.

TABLE 1. Comparison with other circularly polarized ME dipole antennas.

Ref.	Size (λ_0^3)	Feed structure	Impedance bandwidth	Axial-ratio bandwidth	Overlapped bandwidth	Average gain (dBi)
[14]	$0.39 \times 0.39 \times 0.16$	SIW	28.8%	25.9%	25.9%	7.7
[21]	$1.02 \times 0.47 \times 0.29$	L-shaped probe	73.3%	47.7%	47.7%	6.8
[22]	$0.4 \times 0.4 \times 0.25$	Microstrip Line	58.2%	22.5%	22.5%	9.0
[24]	$0.35 \times 0.4 \times 0.25$	SIW	50.0%	36.6%	36.6%	7.7
[26]	$0.82 \times 0.82 \times 0.28$	Microstrip Line	55.3%	42.1%	42.1%	/
Prop.	$\mathbf{0.68 \times 0.48 \times 0.21}$	**Microstrip Line**	**57.0%**	**63.0%**	**57.0%**	**7.2**

seen that W_3 has a great influence on the high frequency resonance point, while the AR performance stays stable in the whole band. The effect of L-shaped strip length L_4 is also studied in Figures 6(i) and (j). When L_4 varies, the impedance matching is slightly affected. For AR, the CP performance of the antenna becomes better, but the AR bandwidth becomes narrower.

3. EXPERIMENTAL RESULTS

To verify the simulated results of the proposed broadband CP ME dipole antenna, it is fabricated as shown in Figure 7. The measured and simulated $|S_{11}|$ of the proposed antenna are plotted in Figure 8(a). It can be seen that the antenna has good impedance matching. And the antenna operates from 2.40 to 4.33 GHz (57%) for $|S_{11}| \leq -10$ dB, which agrees well with simulated results. The measured and simulated ARs of the proposed antenna are plotted in Figure 8(b). The AR bandwidth of the antenna reaches 63%, and the operating frequency band is 2.39 GHz to 4.57 GHz. Figure 8(c) shows the measured and simulated gains at the broadside direction. It can be seen that the antenna gain gradually increases in 2.4–3.6 GHz, and the maximum gain of 7.9 dBi is obtained at 3.6 GHz. In the whole working band, the gain is relatively stable, and the average gain of the antenna is 7.2 dBi.

The simulated and measured radiation efficiencies are given in Figure 8(d). As shown in Figure 8(d), the simulated and measured antenna radiation efficiencies are both better than 77% across the operational frequency region. In the following, the simulated different angle AR of the proposed antenna at key frequencies is provided in Figure 8(e). It can be seen that the CP performance at off-broadside angles and key frequencies remains good, confirming reliable polarization stability in practical scenarios.

Figure 9 shows the E-plane and H-plane radiation patterns of the antenna at 3 GHz, 3.5 GHz, and 4 GHz. It can be seen that the radiation patterns are symmetrical and stable at differ-

ent frequencies over the whole operating band, which demonstrates the superiority of the ME dipole antenna. The RHCP gains of the proposed antenna are 16 dB larger than the left-hand CP (LHCP) gains at broadside direction, which shows that a good RHCP radiation performance is achieved. The measured results are in good agreement with the simulated ones.

A comparison between the proposed design with other existing CP ME dipole antenna elements is listed in Table 1. Compared with other antennas, a wider impedance bandwidth and AR bandwidth is achieved without using a broadband feed network to increase the complexity of the antenna structure [20]. The proposed antenna also has a relatively stable radiation pattern, which is suitable for high-quality wireless communications.

4. CONCLUSION

In this paper, a broadband CP ME dipole antenna with a simple structure is proposed. First, the CP radiation is generated based on the change of the shape and size of the LP antenna. By using the metal column to generate a new magnetic current component and changing the shape of slot etched on the ground plane, the working bandwidth of the antenna at low frequency and high frequency can be expanded respectively. The measured results show that the antenna owns an impedance bandwidth of 57% (2.40–4.33 GHz) and an AR bandwidth of 63% (2.39–4.57 GHz). The antenna could be a good choice for broadband wireless communication system due to the advantage of wide bandwidth, flat gain, and simple structure.

ACKNOWLEDGEMENT

This work was supported in part by the National Natural Science Foundation of China, Grants 62271386, 62301415 and 61901357, Shaanxi Science and Technology Association Youth Talent Lifting Program, Grant 20230149.

REFERENCES

[1] Midya, M., S. Bhattacharjee, and M. Mitra, "Compact CPW-fed circularly polarized antenna for WLAN application," *Progress In Electromagnetics Research M*, Vol. 67, 65–73, 2018.

[2] Santosa, C. E., J. T. S. Sumantyo, C. M. Yam, K. Urata, K. Ito, and S. Gao, "Subarray design for C-band circularly-polarized synthetic aperture radar antenna onboard airborne," *Progress In Electromagnetics Research*, Vol. 163, 107–117, 2018.

[3] Li, C., F.-S. Zhang, F. Zhang, and K. Yang, "A wideband circularly polarized antenna with wide beamwidth for GNSS applications," *Progress In Electromagnetics Research C*, Vol. 84, 189–200, 2018.

[4] Cheng, Y. and Y. Dong, "Wideband circularly polarized split patch antenna loaded with suspended rods," *IEEE Antennas and Wireless Propagation Letters*, Vol. 20, No. 2, 229–233, 2021.

[5] Jiang, H., N. Yan, K. Ma, and Y. Wang, "A wideband circularly polarized dielectric patch antenna with a modified air cavity for Wi-Fi 6 and Wi-Fi 6E applications," *IEEE Antennas and Wireless Propagation Letters*, Vol. 22, No. 1, 213–217, 2023.

[6] Lu, W.-Y., X. Ding, and W. Shao, "Low-profile wide axial-ratio beamwidth circularly polarized antenna with simple feed," *Progress In Electromagnetics Research C*, Vol. 152, 163–170, 2025.

[7] Wang, Z., X. Zhang, H. Fang, A. Ni, and Y. Cheng, "Broadband circularly polarized crossed dipole antenna loaded with magneto-electric dipole," *Progress In Electromagnetics Research C*, Vol. 152, 25–32, 2025.

[8] Wang, J., Y. Zhang, L. Ye, and Q. H. Liu, "A wideband circularly polarized filtering antenna based on slot-patch structure," *IEEE Antennas and Wireless Propagation Letters*, Vol. 22, No. 8, 1858–1862, 2023.

[9] Chen, R.-S., G.-L. Huang, S.-W. Wong, M. K. T. Al-Nuaimi, K.-W. Tam, and W.-W. Choi, "Bandwidth-enhanced circularly polarized slot antenna and array under two pairs of degenerate modes in a single resonant cavity," *IEEE Antennas and Wireless Propagation Letters*, Vol. 22, No. 2, 288–292, 2023.

[10] Wang, L., W.-X. Fang, Y.-F. En, Y. Huang, W.-H. Shao, and B. Yao, "Wideband circularly polarized cross-dipole antenna with parasitic elements," *IEEE Access*, Vol. 7, 35 097–35 102, 2019.

[11] Tan, Q., K. Fan, W. Yu, L. Liu, and G. Q. Luo, "A circularly polarized strip dipole antenna array with working bandwidth above 40% for wireless and satellite communications," *IEEE Antennas and Wireless Propagation Letters*, Vol. 23, No. 1, 9–13, 2024.

[12] Wu, D.-L., J. Pan, L. H. Ye, J.-F. Li, F. Jiang, X. Tian, R. Li, and Z. Hu, "A broadband circularly polarized dipole antenna with high 1 dB gain flatness," *IEEE Antennas and Wireless Propagation Letters*, Vol. 23, No. 6, 1784–1788, 2024.

[13] Luk, K.-M. and H. Wong, "A new wideband unidirectional antenna element," *International Journal of Microwave and Optical Technology*, Vol. 1, No. 1, 35–44, 2006.

[14] Xu, Y., K.-M. Luk, A. Li, and J. Sun, "A novel compact magneto-electric dipole antenna for millimeter-wave beam steering applications," *IEEE Transactions on Vehicular Technology*, Vol. 70, No. 11, 11 772–11 783, 2021.

[15] Zhou, M., Y. Xu, A. Wang, and J. Hou, "A wideband magneto-electric dipole antenna for 4G/5G communication," *Microwave and Optical Technology Letters*, Vol. 65, No. 11, 2941–2946, 2023.

[16] Xu, Y., M. Wang, X. Yang, C. Cui, X. Fan, T. Bai, and J. Hou, "A wideband high-isolated dual-polarized magnetoelectric dipole antenna for 4G/5G communications," *Progress In Electromagnetics Research Letters*, Vol. 122, 53–58, 2024.

[17] Li, Y. and K.-M. Luk, "A 60-GHz wideband circularly polarized aperture-coupled magneto-electric dipole antenna array," *IEEE Transactions on Antennas and Propagation*, Vol. 64, No. 4, 1325–1333, 2016.

[18] Tan, Q., K. Fan, W. Yu, Y. Yu, and G. Q. Luo, "A broadband circularly polarized planar antenna array using magneto-electric dipole element with bent strips for Ka-band applications," *IEEE Antennas and Wireless Propagation Letters*, Vol. 22, No. 1, 39–43, 2023.

[19] Feng, B., L. Li, K. L. Chung, and Y. Li, "Wideband widebeam dual circularly polarized magnetoelectric dipole antenna/array with meta-columns loading for 5G and beyond," *IEEE Transactions on Antennas and Propagation*, Vol. 69, No. 1, 219–228, 2021.

[20] Cui, X., F. Yang, and M. Gao, "Wideband CP magnetoelectric dipole antenna with microstrip line aperture-coupled excitation," *Electronics Letters*, Vol. 54, No. 14, 863–864, 2018.

[21] Li, M. and K.-M. Luk, "A wideband circularly polarized antenna for microwave and millimeter-wave applications," *IEEE Transactions on Antennas and Propagation*, Vol. 62, No. 4, 1872–1879, 2014.

[22] Sun, J. and K.-M. Luk, "Wideband linearly-polarized and circularly-polarized aperture-coupled magneto-electric dipole antennas fed by microstrip line with electromagnetic bandgap surface," *IEEE Access*, Vol. 7, 43 084–43 091, 2019.

[23] Tan, Q., K. Fan, W. Yu, W. Wang, L. Liu, and G. Q. Luo, "A circularly polarized magneto-electric dipole antenna array with wide AR and impedance bandwidth for millimeter-wave applications," *IEEE Antennas and Wireless Propagation Letters*, Vol. 22, No. 9, 2250–2254, 2023.

[24] Tian, Y., J. Ouyang, P. F. Hu, and Y. Pan, "Millimeter-wave wideband circularly polarized endfire planar magneto-electric dipole antenna based on substrate integrated waveguide," *IEEE Antennas and Wireless Propagation Letters*, Vol. 21, No. 1, 49–53, 2022.

[25] Yang, X.-X., H. Qiu, T. Lou, Z. Yi, Q.-D. Cao, and S. Gao, "Circularly polarized millimeter wave frequency beam scanning antenna based on aperture-coupled magneto-electric dipole," *IEEE Transactions on Antennas and Propagation*, Vol. 70, No. 9, 7603–7611, 2022.

[26] Ding, K., Y. Li, and Y. Wu, "Broadband circularly polarized magnetoelectric dipole antenna by loading parasitic loop," *IEEE Transactions on Antennas and Propagation*, Vol. 70, No. 11, 11 085–11 090, 2022.